Synthesis and Spectral Properties of Nanocrystalline V-Substituted In₂S₃, a Novel Material for More Efficient Use of Solar Radiation

Raquel Lucena,[†] Irene Aguilera,[‡] Pablo Palacios,[‡] Perla Wahnón,[‡] and José C. Conesa*,[†]

Instituto de Catálisis y Petroleoquímica, CSIC, Marie Curie 2, Cantoblanco, 28049 Madrid, Spain, and Instituto de Energía Solar & Dept. Tecnologías Especiales, ETSI de Telecomunicación, Universidad Politécnica de Madrid, Ciudad Universitaria, 28040 Madrid, Spain

Current photovoltaic (PV) devices and photocatalysts can use solar light through a process in which the absorption of one photon by a semiconductor leads in the latter to the promotion of an electron from the valence band (VB) to the conduction band (CB) with the subsequent production of electric current or chemical reactions. Within this mechanism, photons with energy lower than the forbidden band gap width E_g cannot be used. In recent years it has been proposed[1] that the insertion of an additional level (the intermediate band, IB) in the forbidden gap could provide an additional path for attaining the same final excitation result through the absorption of two photons with energy lower than E_g, similarly to what happens in natural photosynthesis (Figure 1). Photogenerated holes and electrons are then extracted from the VB and CB at the corresponding electron potential: in a photovoltaic cell, with electrical contacts (thick black lines in Figure 1a) having proper Fermi levels, and in photocatalysis, via transfer to adsorbed molecules having proper redox states, driving chemical reactions.

Thus a larger number of photogenerated charge carriers would be available for producing electric current or chemical processes without decreasing the voltage or chemical potential of the photogenerated charge carriers, and the solar spectrum would be more thoroughly and efficiently used. In photovoltaics, for example, this would lead to an ideal upper limit of the efficiency in solar energy use of around 63%, while with a normal semiconductor this upper limit would be approximately 41%.[1] It should be noted that this type of electronic structure could also be useful in other applications, for example, photon up- or down-converters or new types of IR detectors.

To achieve the desired performance, the electronic structure of the targeted IB material should have some specific features in addition to the level ordering depicted in Figure 1a. The intermediate level should be a truly delocalized band (even if relatively narrow), not a discrete localized level, to minimize undesirable nonradiative recombination.[2] It should not overlap the CB nor the VB, to prevent the electron or
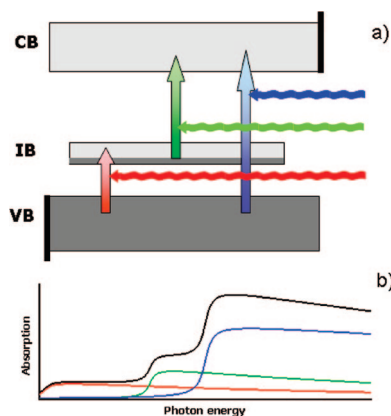

Figure 1. Intermediate band (IB) working principle: (a) photons of different wavelengths promote electrons from the valence band (VB) directly to the conduction band (CB) and also from the VB to the IB and from the IB to the CB. (b) A wider photon energy range is thus used.

hole deexcitation to the IB through thermalization (which would waste energy), and should be partially occupied by electrons so that both low energy transitions (from the VB to this intermediate band, IB, and from the IB to the CB) may occur at comparable rates, as is required in this scheme. Finally, the VB−CB gap should be close to 2.0 eV to reach the maximum photovoltaic efficiency.[1] To our knowledge, no compound has been made until now which fulfills all the required IB features.

In previous works[3–5] we proposed, based on density functional theory (DFT) calculations, that tetrahedral semiconductors including certain transition metals (TM) could be valid IB materials. Here we change the approach and start from a semiconductor containing octahedral cation positions, where substitution by a TM is likely to be more favorable, and undertake the synthesis (in nanocrystalline powder form) and optical characterization of this TM-substituted material, obtaining spectral results that confirm the expectations from DFT. To our knowledge this is the first time that a compound, predicted with DFT calculations to have the desired IB characteristics, is synthesized and shows experimental features agreeing with the computed electronic structure.

In₂S₃ is a semiconductor with a direct bandgap $E_g \approx 2.0$ eV wide[6] having in its most stable β phase a defect spinel structure with cation vacancies ordered in the tetrahedral sites, producing a body-centered tetragonal structure (space group $I4_1/amd$; see Figure S1 in the Supporting Information).[7] Most of the indium in it (75%) has thus octahedral coordination. In₂S₃ is frequently used as a window layer material in thin film PV cells so that the preparation methods, well adapted to PV cell manufacture, are already known for

---

[†] Instituto de Catálisis, CSIC.
[‡] Instituto de Energía Solar, UPM.
(1) Luque, A.; Martí, A. *Phys. Rev. Lett.* **1997,** *78,* 5014.
(2) Luque, A.; Martí, A.; Antolín, E.; Tablero, C. *Phys. B: Condens. Matter* **2006,** *382,* 320.

(3) Wahnón, P.; Palacios, P.; Fernández, J. J.; Tablero, C. *J. Mater. Sci.* **2005,** *40,* 1383.
(4) Palacios, P.; Fernández, J. J.; Sánchez, K.; Conesa, J. C.; Wahnón, P. *Phys. Rev. B* **2006,** *73,* 085206.
(5) Palacios, P.; Sánchez, K.; Conesa, J. C.; Fernández, J. J.; Wahnón, P. *Thin Solid Films* **2007,** *515,* 6280.
(6) Kambas, K.; Anagnostopoulos, A.; Ves, S.; Ploss, B.; Spyridelis, J. *Phys. Status Solidi B* **1985,** *127,* 201.
(7) Steigmann, G. A.; Sutherland, H. H.; Goodyear, J. *Acta Crystallogr.* **1965,** *19,* 967.
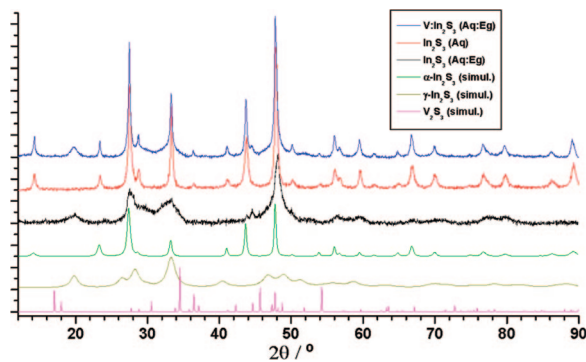
Figure 2. Powder X-ray diffractograms of the materials obtained: In₂S₃ (solvothermally made in water or water/ethylene glycol mixture) and V-doped In₂S₃ (made in water/ethylene glycol). Simulated diffractograms of α- and γ-In₂S₃ (with fitted linewidths) and V₂S₃ are also shown.

it. Furthermore, sulfides based on octahedral indium have shown good photocatalytic properties,[8] and the photoelectrochemical properties of In_2S_3 have been characterized.[9] In_2S_3 seems thus a good candidate to make an IB material through substitution of In by a TM, especially when aiming at photovoltaic applications. We initially chose Ti and V as TM dopants. These elements could form an IB from the lowest subshell (threefold degenerate in octahedral symmetry) of their 3d levels and, acting as trivalent substituents, would provide one and two electrons respectively to this IB, leaving it therefore partially occupied as required. We describe here the most promising results, obtained using vanadium as the dopant.

The polycrystalline In_2S_3 material obtained hydrothermally in aqueous solution displays a powder X-ray diffractogram (XRD; Figure 2) where all peaks correspond to the cubic α phase of In_2S_3,[10] having the same structure as the mentioned β phase but with the cation vacancies disordered. A crystallite size of around 23 nm can be obtained from the peak widths by applying Scherrer's formula, while the peak positions give a cell parameter of $a = 10.75$ Å, close to the literature value (10.774 Å[10]). The reaction leading to this product can be written as

$$2InCl_3 + 3Na_2S \rightarrow In_2S_3 + 6NaCl \qquad (1)$$
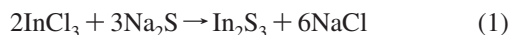
Its diffuse reflectance (DR) UV−visible−near IR (NIR) spectrum was also obtained (see Supporting Information, Figure S2). The Kubelka−Munk[11] transform function of the reflectance R (KM = $(1 - R)^2/(2R)$), which gives the ratio of the absorption and scattering coefficients, is shown in Figure 3a. It rises steeply above 2.0 eV, in accordance with the direct band gap of In_2S_3.

When trying to prepare the vanadium doped material in a similar way, a substantial oxidation of this element to V^{IV},
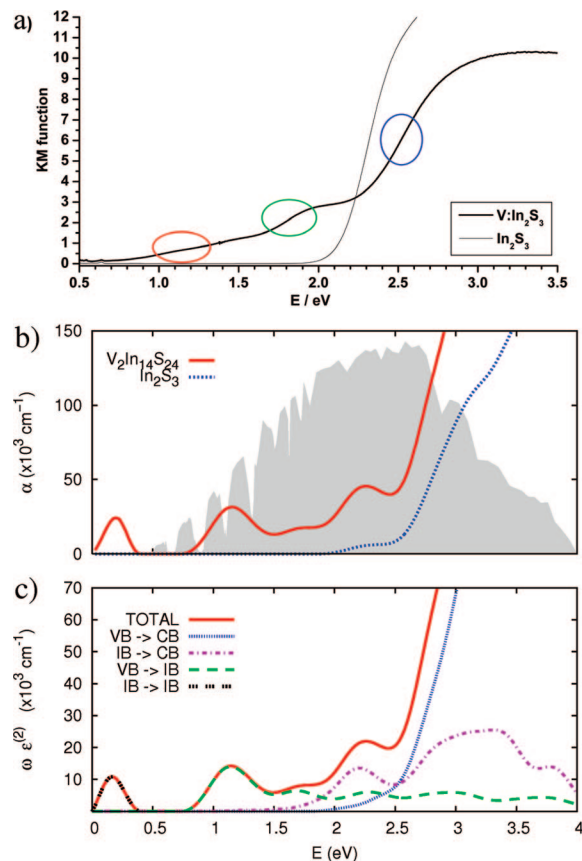

Figure 3. (a) UV−vis−NIR DR data obtained for well-crystallized In₂S₃ and V-containing In₂S₃. Ovals highlight the contributions ascribed to the different transitions shown in Figure 1. (b) Absorption coefficient computed with DFT for both systems. The AM1.5G solar spectrum is drawn as the background, to show the improved range of its absorption that would be achieved with the new material. (c) Detail of the contributions of the different transitions to the optical properties (ω-weighted imaginary part of the dielectric function ε) of V-substituted In₂S₃.

probably ascribable to the large concentration of protons present, was detected using EPR spectroscopy. The problem was alleviated by using a water−ethylene glycol mixture as solvent. As shown in Figure 2, when preparing In_2S_3 this led to an ill-crystallized product (with a small broad peak at $2\theta \approx 19.8°$ indicating the simultaneous formation of the less stable hexagonal γ phase of In_2S_3, which has also most or all of In ions in octahedral coordination[12]) which had optical characteristics otherwise quite similar to those of the former sample. However, it gave a better crystallized V-doped material (its sharp XRD peaks indicate a particle size around 20 nm) having an atomic ratio V:In = 0.093 according to chemical analysis. No new XRD peak (in particular, features due to a V_2S_3 phase[13] are absent) appears in it beyond those observed in the In_2S_3 preparations, indicating that a separate V-containing phase has not been formed. TEM data with EDS analysis (see Supporting Information, Figure S3) confirms that the desired incorporation of vanadium into In_2S_3, never reported previously, seems indeed to have taken place.

The EPR spectrum of this material (see Supporting Information, Figure S4) shows a signal at $g \approx 1.98$, with

(8) (a) Kale, B. B.; Baeg, J.-O.; Lee, S. M.; Chang, H.; Moon, S.-J.; Lee, C.-W. *Adv. Funct. Mater.* **2006**, *16*, 1349. (b) Lei, Z.; You, W.; Liu, M.; Zhou, G.; Takata, T.; Hara, M.; Domen, K.; Li, C. *Chem. Commun.* **2003**, 2142. (c) Yu, X. D.; Qu, X. S.; Guo, I. H.; Hu, C. W. *Chin. Chem. Lett.* **2005**, *16*, 2005.
(9) (a) Becker, R. S.; Zheng, T.; Elton, J.; Saeki, M. *Solar Energy Mater.* **1986**, *13*, 97. (b) Herrasti, P.; Fatás, E.; Herrero, J.; Ortega, J. *Electrochim. Acta* **1990**, *35*, 345.
(10) (a) Adenis, C.; Olivier-Fourcade, J.; Jumas, J. C.; Philippot, E. *Rev. Chim. Minérale* **1987**, *24*, 10. (b) JCPDS file 32-0456.
(11) Dupuis, G.; Menu, M. *Appl. Phys. A: Mater. Sci. Process.* **2006**, *83*, 469.

(12) (a) Diehl, R.; Nitsche, R. *J. Cryst. Growth* **1973**, *20*, 38. (b) Diehl, R.; Carpentier, C. D.; Nitsche, R. *Acta Crystallogr., B* **1976**, *32*, 1257.
(13) Ohno, Y.; Watanabe, H.; Kawata, A.; Nakai, S.; Sugiura, C. *Phys. Rev. B* **1982**, *25*, 815.

Communications

Chem. Mater., Vol. 20, No. 16, 2008 5127

some superimposed hyperfine structure; these features are indicative of V^{IV} species (V^{V} and V^{III} are not detectable in these spectra). Spectrum integration (carried out as explained in the Supporting Information) shows that V^{IV} represents approximately 25% of the total vanadium content. This result, together with the synthesis conditions used, indicates that most of the vanadium remains as V^{III}. Its incorporation in the product as a sulfide would follow a reaction similar to eq 1 above.

The DR spectrum of this V-doped material was obtained (Figure S2 of the Supporting Information); Figure 3a shows its Kubelka−Munk transform. Besides the main absorption edge at $E \approx 2.1$ eV, two new main features appear: a distinct shoulder or step starting at approximately 1.6 eV and a broad absorption that starts at rather low energy, possibly around 0.7 eV, and increases steadily until meeting the other feature at approximately 1.6 eV.

According to detailed quantum calculations, which are described elsewhere,[14] DFT predicts for β-In$_2$S$_3$ (the ordered version of α-In$_2$S$_3$) a bandgap of 0.8 eV, lower than the experimental one as is typical in calculations at this theory level. The VB and CB are constituted mainly by S 2p and In 5s orbitals, respectively, as shown in earlier quantum mechanical studies of In thiospinels.[15] The calculations made in the mentioned work (see the description of procedures and models in the Supporting Information) show that, upon substitution of octahedral In by V, a well-defined, fully spin-polarized IB appears in the semiconductor gap (Figure S5 of the Supporting Information); this IB is mainly made up of V 3d orbitals, has three electronic levels per vanadium atom, and contains two electrons per vanadium atom. This is what would be expected for a system based on the formal redox state V^{III}, which in a perfect octahedral coordination would contain two electrons in the triply degenerate t_{2g} manifold. Similar calculations were made also for the γ-In$_2$S$_3$ phase, with or without V, and gave energy levels and gaps with values and features (not shown here) quite similar to those found for β-In$_2$S$_3$. The conclusions do not depend thus on whether V lies in the α or γ phase. From these DFT data the corresponding optical absorption spectrum can be predicted; the result, compared with that obtained in the same way for nondoped β-In$_2$S$_3$, is given in Figure 3b, and can be analyzed examining the different contributions to the imaginary part of the dielectric function (from which the absorption value is calculated) as shown in Figure 3c.

These curves show for V-doped In$_2$S$_3$ an absorption in a range below 0.5 eV (resulting from electronic transitions within the IB) and two increases in absorption starting at about 0.7 eV (resulting from transitions from the VB to the empty IB states) and 1.5 eV (resulting from transitions from the occupied IB states to the CB), respectively, besides the jump edge at approximately 2.0 eV resulting from VB−CB transitions. For pure In$_2$S$_3$, as expected, only the excitation due to the VB−CB transitions appears. The features observed for V-doped In$_2$S$_3$ match the essential ones of the experi-

mental result in Figure 3a nicely, allowing the latter to be interpreted as resulting from the presence of all three transitions detailed in Figure 1. The fact that the sub-bandgap features in the calculated spectrum are peak-like while those in the experimental one are more step-like may be explained by disorder or considering that the experimental observation will include phonon-assisted photon absorptions (indirect transitions) that cannot be reproduced using the current calculation method.

The observation of both sub-bandgap features in Figure 3a indicates that the IB of the material is partially filled as predicted theoretically. If it were empty or completely filled one of the two transitions would be absent. This could have occurred in previous work on highly mismatched semiconductor alloys,[16] which reported only two absorption features.

The evidence of solid solution formation given by XRD and the agreement between predicted and experimental absorption spectra show the realization of the IB scheme proposed for high efficiency PV cells in a single-phase compound for the first time. As said previously, a number of applications could benefit from this type of material. More efficient photovoltaic cells could be achieved; new photo-catalysts or photoelectrochemical materials could allow photosyntheses or pollutant destruction to take place using solar energy more efficiently; new photon up-converters or down-converters, or improved IR detectors, could come about; and magnetic half-metals useful in spintronics could be conceived. Furthermore, a variety of spinel-type or layered sulfide phases exist which contain octahedrally coordinated In[17] and thus may allow fine-tuning of properties in TM-substitution-based IB materials. Further work is under way for the experimental characterization of the synthesized material and for the preparation of similar ones, as well as for the verification of their photocatalytic activity and the assembly of PV cells based on such systems. The effective obtention of higher efficiencies in these applications through the use of this family of compounds remains the main challenge in such a study.

Supporting Information Available: Experimental details, DFT calculation methods and models, TEM data, EPR, UV−vis−NIR diffuse reflectance spectra, and DOS curves (PDF file). This material is available free of charge via the Internet at http://pubs.acs.org.

CM801128B

(14) Palacios, P.; Aguilera, I.; Sánchez, K.; Conesa, J. C.; Wahnón, P. *Phys. Rev. Lett.* **2008**, accepted.

(15) Marinelli, M.; Baroni, S.; Meloni, F. *Phys. Rev. B* **1988**, *38*, 8258.

(16) (a) Yu, K. M.; Walukiewicz, W.; Wu, J.; Shan, W.; Beeman, J. W.; Scarpulla, M. A.; Dubon, O. D.; Becla, P. *J. Appl. Phys.* **2004**, *95*, 6232. (b) Yu, K. M.; Walukiewicz, W.; Ager, J. W.; Bour, D.; Farshchi, R.; Dubon, O. D.; Li, S. X.; Sharp, V.; Haller, E. E. *Appl. Phys. Lett.* **2006**, *88*, 092110.

(17) Haeuseler, H.; Srivastava, S. K. *Z. Kristallogr.* **2000**, *215*, 205.